Electronic Supplementary Material (ESI) for Physical Chemistry Chemical Physics.

Supplementary Information

Molecular origins of the multi-donor strategy in inducing bathochromic shifts and enlarging Stokes shifts of fluorescent proteins

Xia Wu,[a] Davin Tan,[a] Qinglong Qiao,[b] Wenting Yin,[b] Zhaochao Xu,*[b] Xiaogang Liu*[a]

a. Fluorescence Research Group, Singapore University of Technology and Design, 8 Somapah Road, Singapore, 487372, Singapore; E-mail: xiaogang_liu@sutd.edu.sg.

b. CAS Key Laboratory of Separation Science for Analytical Chemistry, Dalian Institute of Chemical Physics, Chinese Academy of Sciences, 457 Zhongshan Road, Dalian 116023, China; E-mail: zcxu@dicp.ac.cn

Contents

1. The Model of the *t* index

D_{CT} is defined as:

$D_{CT} = |R_+ - R_-|$

where the R_+ and R_- refer to the centroid of the electron and hole, respectively. D_{CT} increases when the hole and electron become further separated.

H index is defined by the relation:

$$H = \frac{|\sigma_{ele}| + |\sigma_{hole}|}{2}$$

where σ_{ele}, σ_{hole} refer to the distribution breadth index of the electron and the hole, respectively . When the *H* index becomes larger, the average extension of the hole and the electron in charge transfer direction gets larger.

The *t* index represents the difference between D_{CT} and *H*:

$t = D_{CT} - H$

whereby a larger *t* index corresponds to a higher degree of ICT.[1, 2]

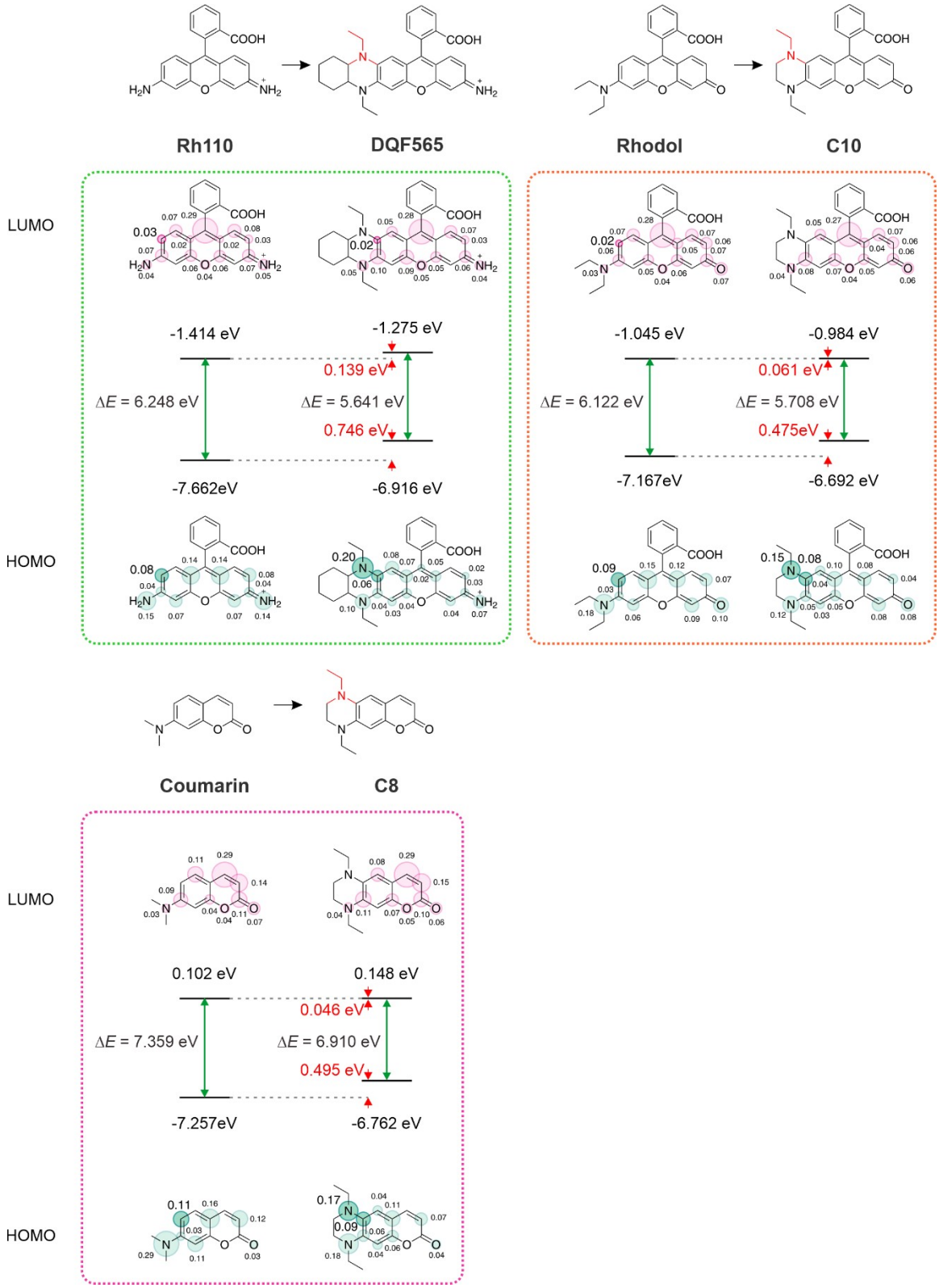

Fig. S1 The energy levels of HOMO and LUMO and the corresponding electronic gaps (ΔE) of small molecule fluorophores based on the multi-donor strategy in water.

Table S1. Calculated/experimental peak UV-vis absorption wavelength (λ_{abs}), peak emission wavelength (λ_{em}), Stokes shift ($\Delta\lambda$), oscillator strength (f), and t-index of small molecule fluorophores based on the multi-donor strategy in water.

Fluorophore	λ_{abs} (nm)	λ_{abs} (Exp) (nm)	λ_{em} (nm)	λ_{em} (Exp) (nm)	$\Delta\lambda$ (nm)	$\Delta\lambda$ (Exp) (nm)	f	t index (Å)
Rh110	392	564[a]	413	587[a]	21	23[a]	0.7215	-1.219
DQF565	482	593[a]	597	653[a]	115	60[a]	0.3419	-0.858
Rhodol	405	520[b]	446	550[b]	41	30[b]	0.7728	-1.460
C10	461	520[c]	583	666[c]	122	146[c]	0.3850	-1.206
Coumarin	317	373[d]	352	446[d]	35	73[d]	0.5721	-0.655
C8	354	410[e]	454	552[e]	100	142[e]	0.2443	-0.014

[a]Experiments data are extracted from literature.[3]

[b]Experiments data are extracted from literature.[4]

[c]Experiments data are extracted from literature.[5]

[d]Experiments data are extracted from literature.[6]

[e]Experiments data are extracted from literature.[7]

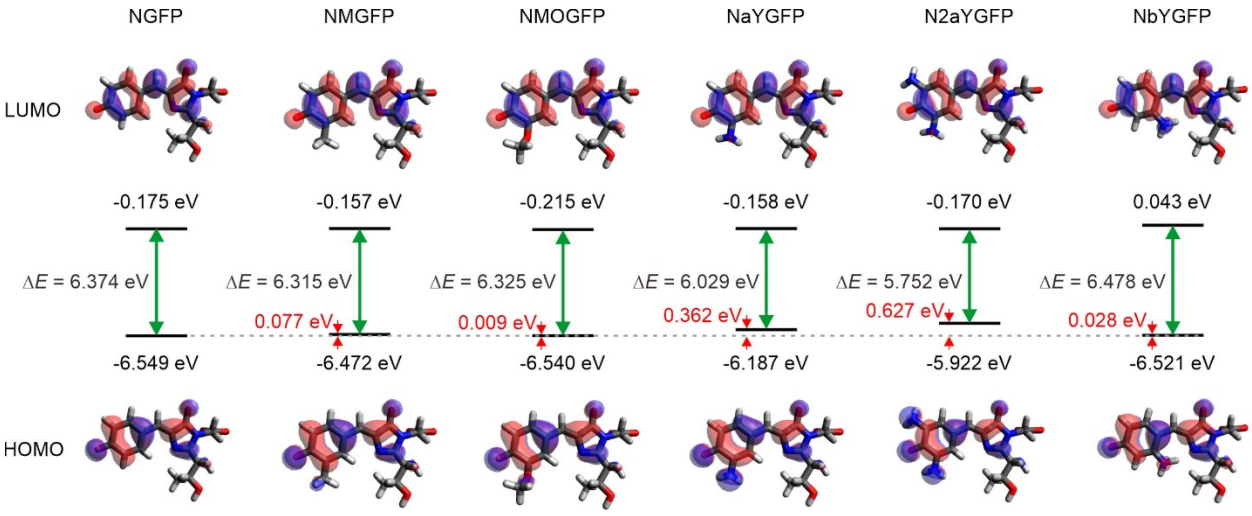

Fig. S2 Frontier molecular orbitals and electronic transitions of the NGFP analogues.

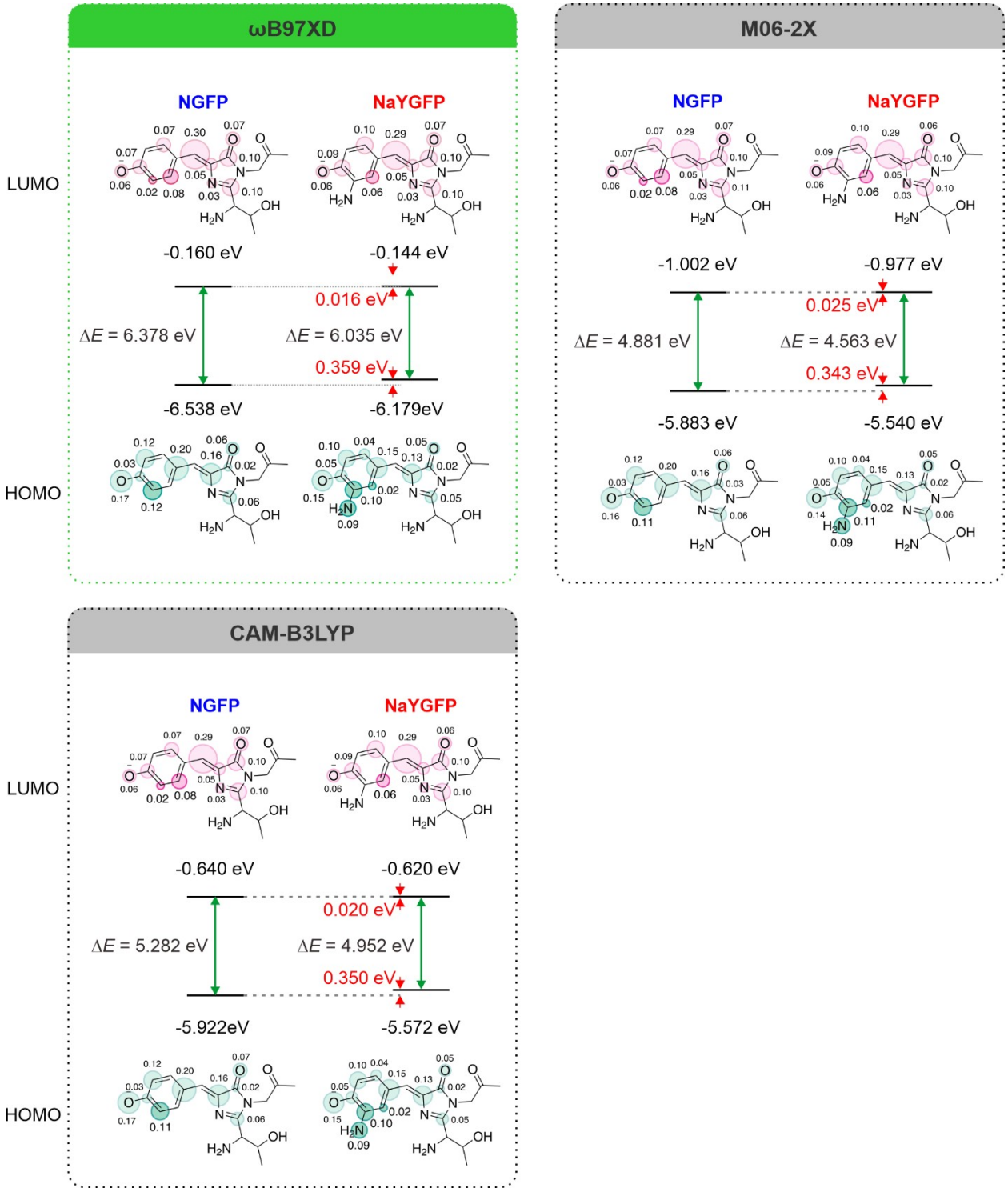

Fig. S3 The energy levels of HOMO and LUMO and the corresponding electronic gaps (ΔE) of NGFP and NaYGFP calculated using different functionals with the Def2svp basis set in water.

Table S2. Calculated peak UV-vis absorption wavelength (λ_{abs}), peak emission wavelength (λ_{em}), Stokes shift ($\Delta\lambda$), oscillator strength (*f*), and *t*-index of the NGFP and NaYGFP using different functionals with the Def2svp basis set in water.

Functional	NGFP					NaYGFP				
	λ_{abs} (nm)	λ_{em} (nm)	$\Delta\lambda$ (nm)	*f*	*t* index (Å)	λ_{abs} (nm)	λ_{em} (nm)	$\Delta\lambda$ (nm)	*f*	*t* index (Å)
CAM-B3LYP	371	398	27	0.9965	-1.987	398	469	71	0.6246	-0.996
M06-2X	376	403	27	0.9798	-2.001	401	465	64	0.6740	-0.910
ωB97XD	371	400	30	0.9810	-1.933	398	474	76	0.6093	-0.868

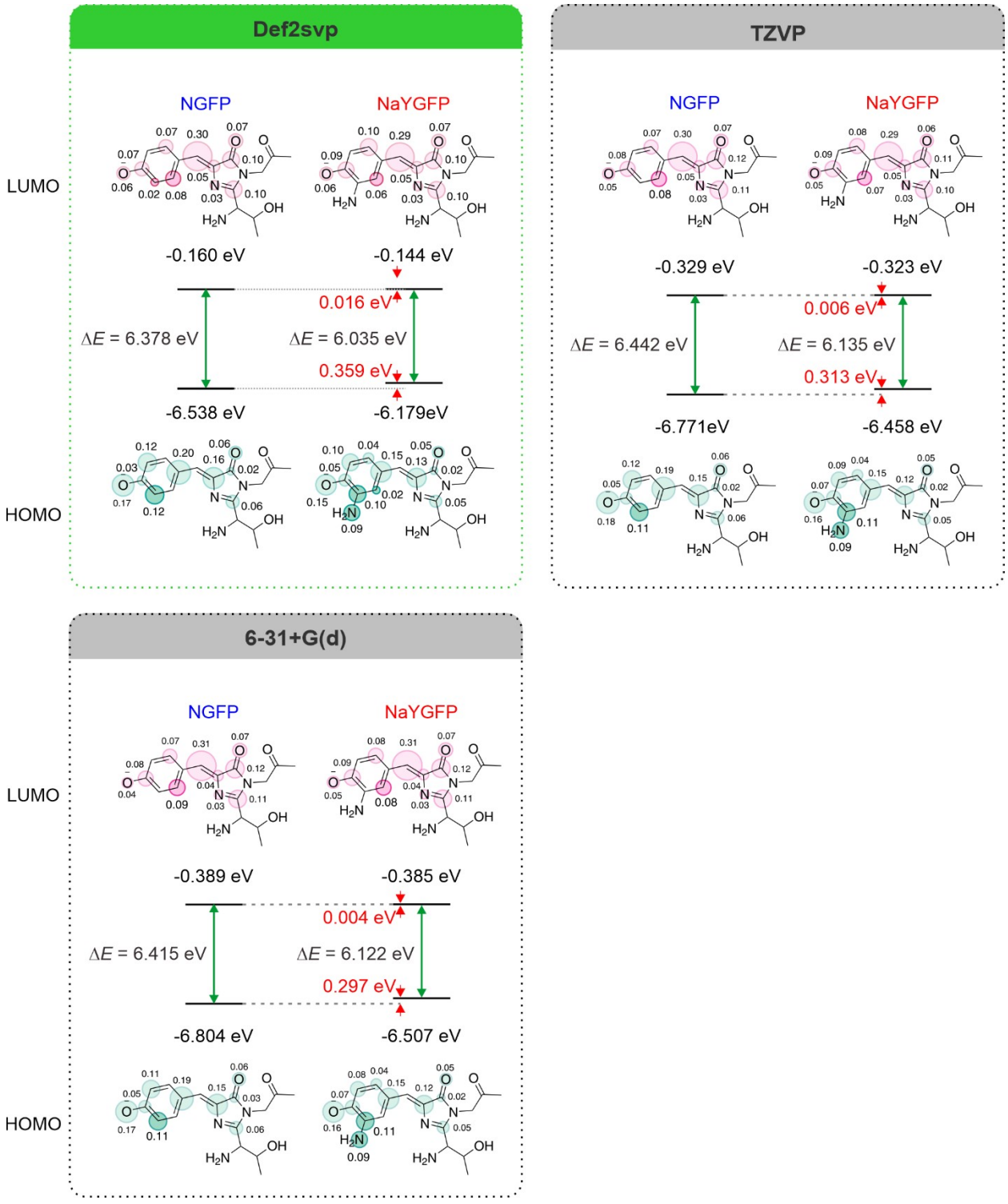

Fig. S4 The energy levels of HOMO and LUMO and the corresponding electronic gaps (ΔE) of NGFP and NaYGFP calculated using different basis sets with the ωB97XD functional in water.

Table S3. Calculated peak UV-vis absorption wavelength (λ_{abs}), peak emission wavelength (λ_{em}), Stokes shift ($\Delta\lambda$), oscillator strength (*f*), and *t*-index of the NGFP and NaYGFP using different basis sets with the ωB97XD functional in water.

	NGFP					NaYGFP				
Basis set	λ_{abs} (nm)	λ_{em} (nm)	$\Delta\lambda$ (nm)	*f*	*t* index (Å)	λ_{abs} (nm)	λ_{em} (nm)	$\Delta\lambda$ (nm)	*f*	*t* index (Å)
6-31+G(d)	377	412	35	0.9792	-1.883	400	459	59	0.7795	-1.054
TZVP	373	408	35	0.9635	-1.905	397	466	69	0.6996	-1.013
Def2svp	371	400	30	0.9810	-1.933	398	474	76	0.6093	-0.868

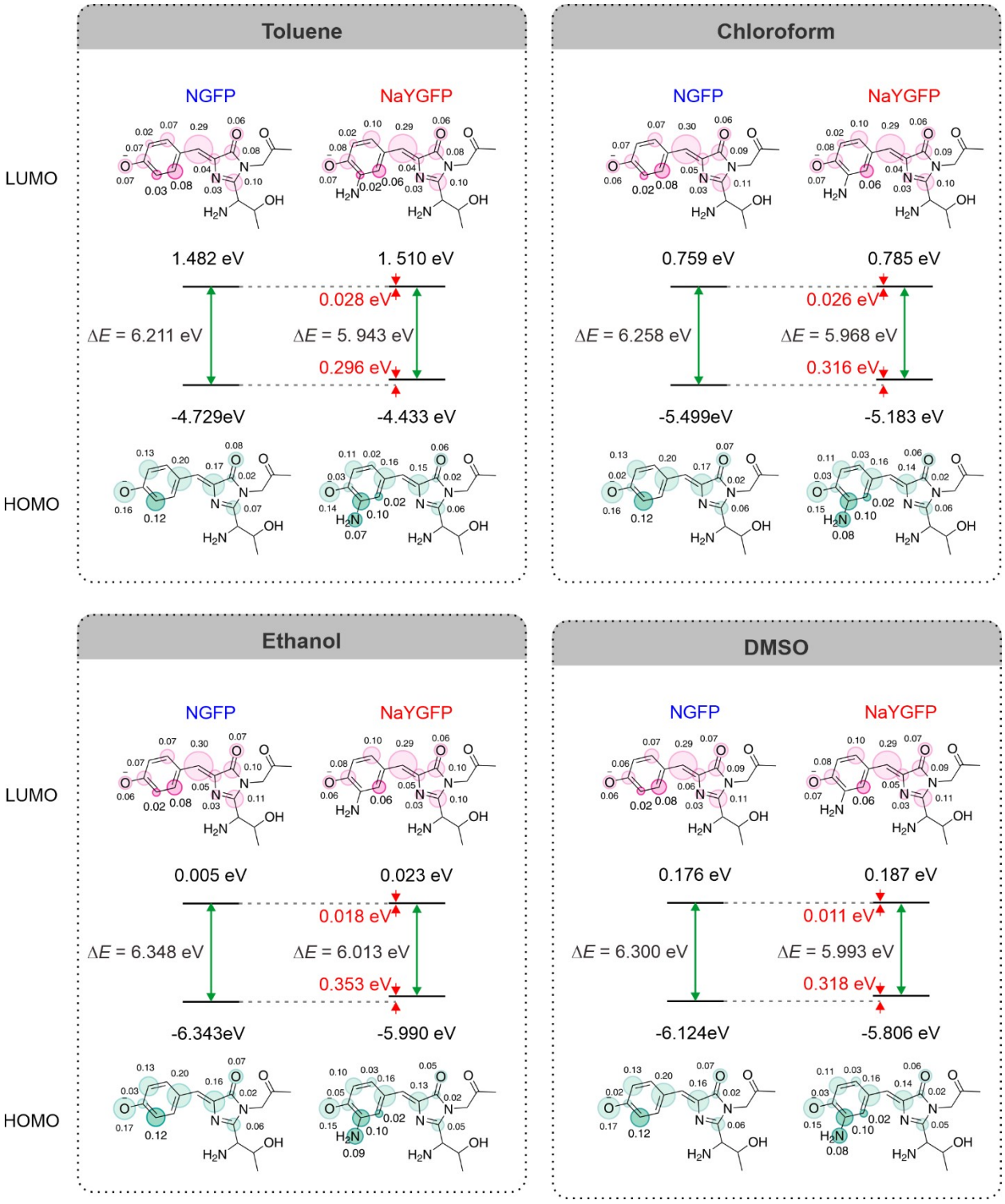

Fig. S5 The energy levels of HOMO and LUMO and the corresponding electronic gaps (ΔE) of NGFP and NaYGFP in different solvents. Note that we employed the deprotonated phenol groups in all these calculations, to focus on the impact of the solvent polarity on the spectral shifts. The protonation-deprotonation equilibrium could also affect the fluorescence properties of these fluorophores. However, this discussion is beyond the scope of our current manuscript.

Table S4. Calculated peak UV-vis absorption wavelength (λ_{abs}), peak emission wavelength (λ_{em}), Stokes shift ($\Delta\lambda$), oscillator strength (*f*), and *t*-index of the NGFP and NaYGFP in different solvents.

Solvent	NGFP					NaYGFP				
	λ_{abs} (nm)	λ_{em} (nm)	$\Delta\lambda$ (nm)	*f*	*t* index (Å)	λ_{abs} (nm)	λ_{em} (nm)	$\Delta\lambda$ (nm)	*f*	*t* index (Å)
Toluene	383	406	23	0.9927	-1.95	405	444	39	0.8472	-1.140
Chloroform	379	405	26	0.9906	-1.953	403	448	45	0.8060	-1.117
Ethanol	373	402	29	0.9826	-1.931	400	467	67	0.6653	-1.025
DMSO	376	405	29	0.9808	-1.975	400	457	57	0.7699	-1.160
Water	371	400	30	0.9810	-1.933	398	474	76	0.6093	-0.868

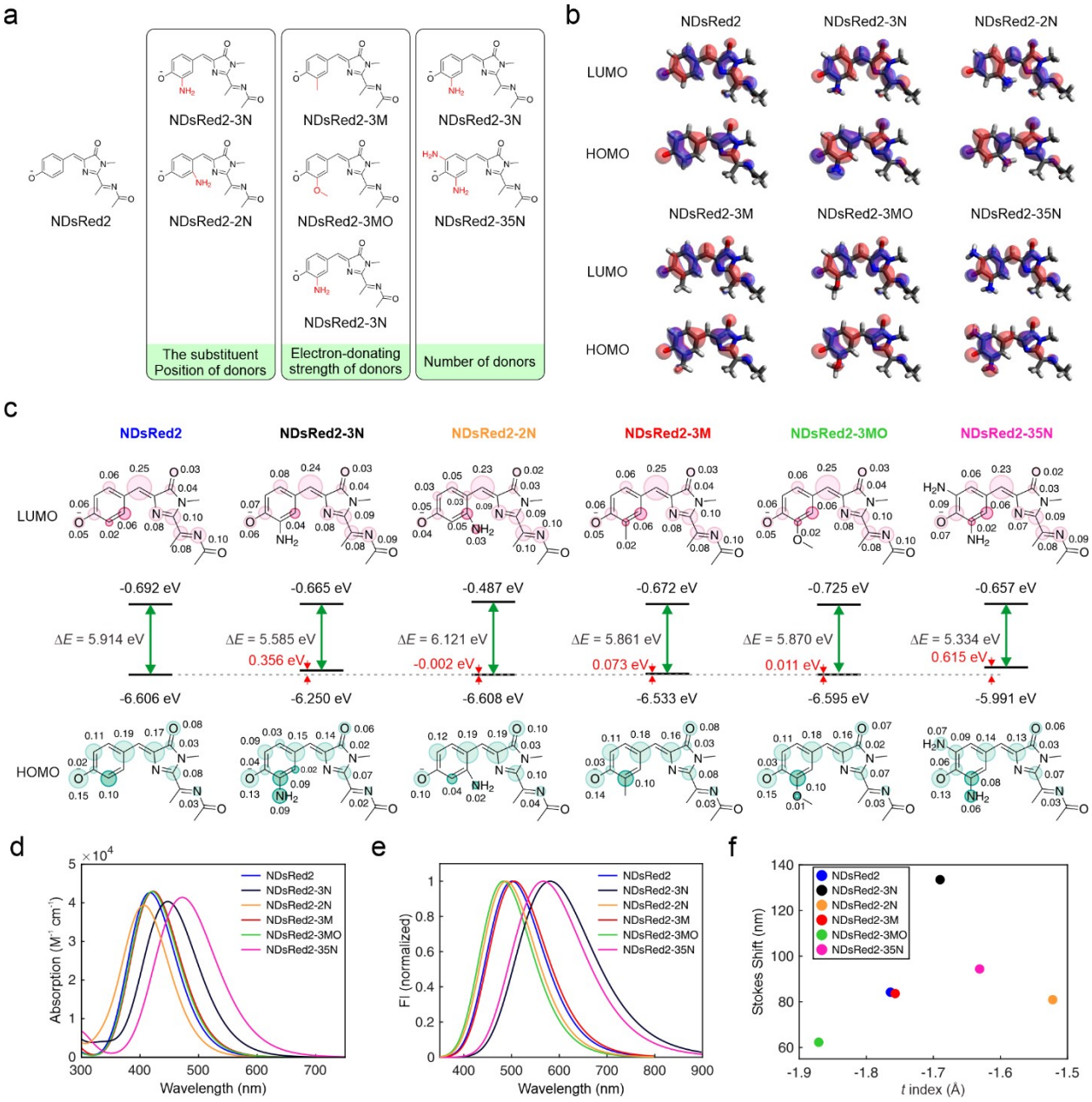

Fig. S6 (a) Chemical structures and (b) atomic contributions to the charge density distributions in the LUMO and HOMO and (c) the energy levels of HOMO and LUMO and the corresponding electronic gaps (ΔE), calculated (d) UV-vis absorption, (e) normalized emission spectra, and (f) the Stokes shifts as a function of the *t* index in the DeRed2 analogues in water.

Table S5. Calculated/experimental peak UV-vis absorption wavelength (λ_{abs}), peak emission wavelength (λ_{em}), Stokes shift ($\Delta\lambda$), oscillator strength (*f*), and *t*-index of the DeRed2 fluorophore analogues in water.

Fluorophore analogues	λ_{abs} (nm)	λ_{abs} (nm)[a)]	λ_{em} (nm)	λ_{em} (nm)[a)]	SS (nm)	SS (nm)[a)]	*f*	*t* index (Å)
NDsRed2	417	561	501	587	84	26	1.0302	-1.764
NDsRed2-3M	423		506		83		1.0357	-1.757
NDsRed2-3MO	421		483		62		1.0235	-1.871
NDsRed2-3N	447		581		134		0.7567	-1.690
NDsRed2-35N	472		567		95		1.0108	-1.631
NDsRed2-2N	408		489		81		0.9991	-1.522

[a)] Experimental data derived from previous works.[8]

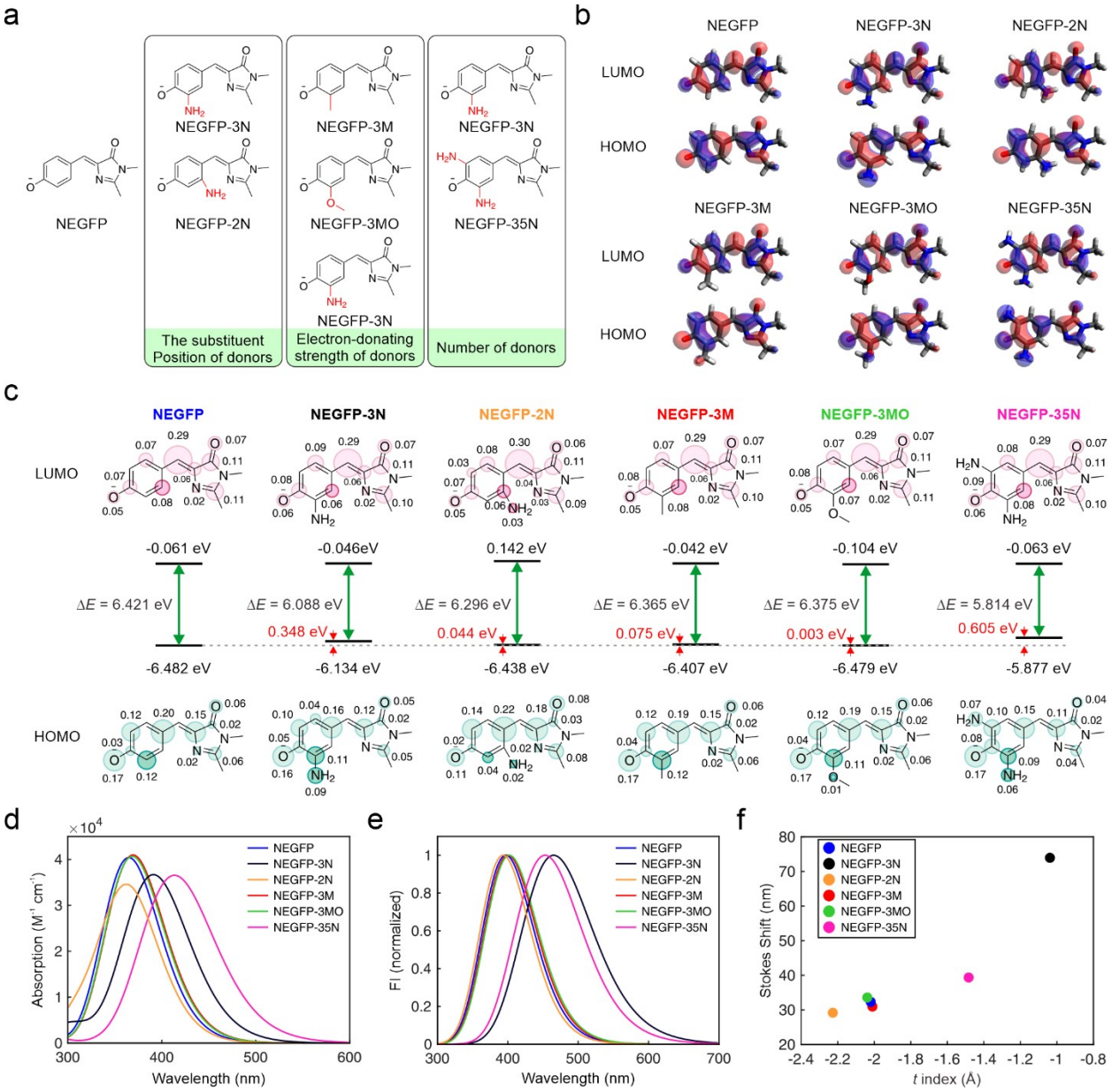

Fig. S7 (a) Chemical structures and (b) atomic contributions to the charge density distributions in the LUMO and HOMO and (c) the energy levels of HOMO and LUMO and the corresponding electronic gaps (ΔE), calculated (d) UV-vis absorption, (e) normalized emission spectra, and (f) the Stokes shifts as a function of the *t* index in the EGFP analogues in water.

Table S6. Calculated/experimental peak UV-vis absorption wavelength (λ_{abs}), peak emission wavelength (λ_{em}), Stokes shift ($\Delta\lambda$), oscillator strength (*f*), and *t*-index of the EGFP fluorophore analogues in water.

Fluorophore analogues	λ_{abs} (nm)	λ_{abs} (nm)[a)]	λ_{em} (nm)	λ_{em} (nm)[a)]	SS (nm)	SS (nm)[a)]	*f*	*t* index (Å)
NEGFP	365	488	397	507	32	19	0.9701	-2.019
NEGFP-3M	369		400		31		0.9883	-2.010
NEGFP-3MO	369		402		33		0.9911	-2.038
NEGFP-3N	391		465		74		0.6192	-1.038
NEGFP-35N	414		453		39		0.8683	-1.483
NEGFP-2N	364		393		29		0.7977	-2.227

[a)] Experimental data derived from previous works.[8]

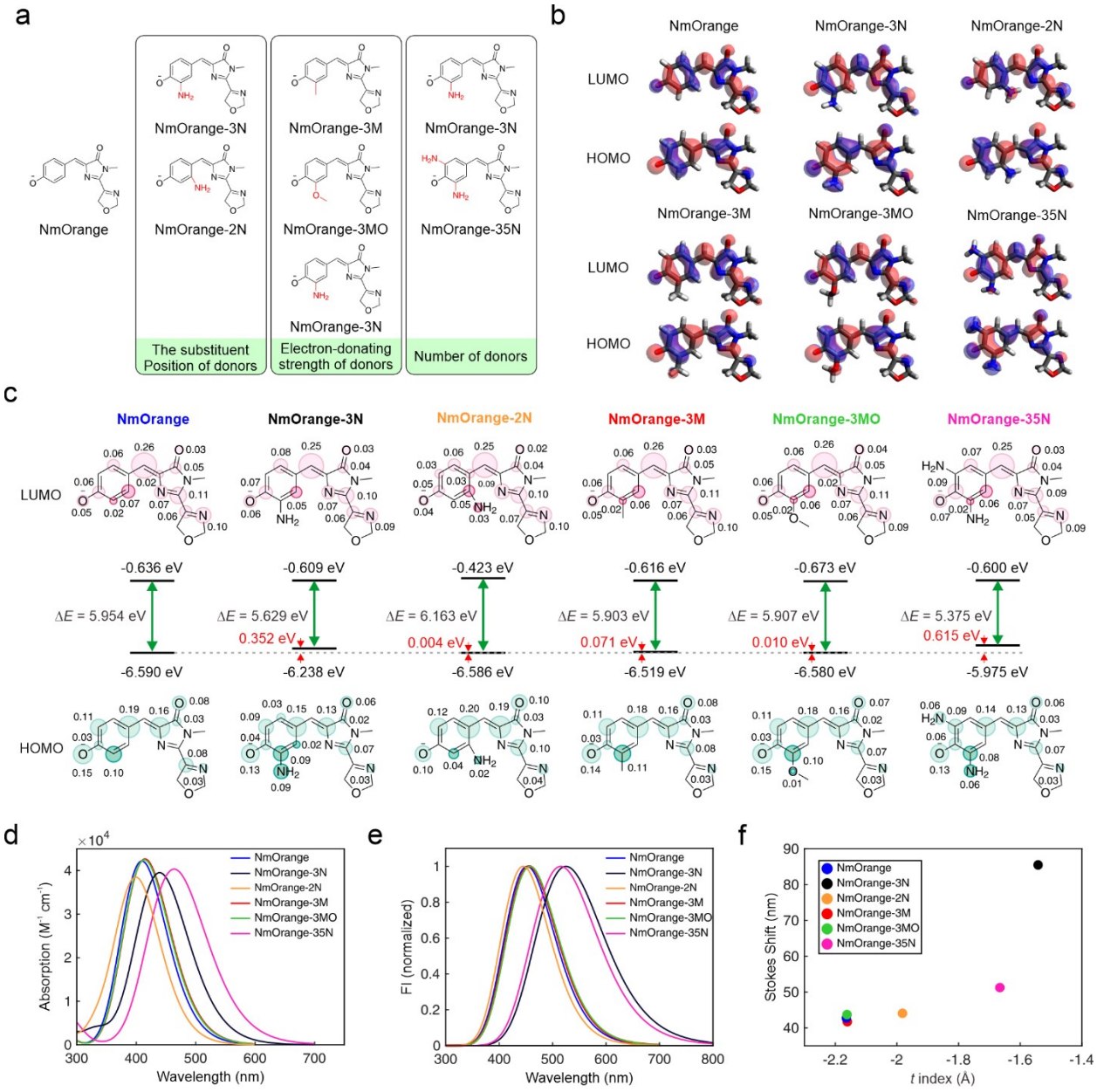

Fig. S8 (a) Chemical structures and (b) atomic contributions to the charge density distributions in the LUMO and HOMO and (c) the energy levels of HOMO and LUMO and the corresponding electronic gaps (ΔE), calculated (d) UV-vis absorption, (e) normalized emission spectra, and (f) the Stokes shifts as a function of the *t* index in the mOrange analogues in water.

Table S7. Calculated/experimental peak UV-vis absorption wavelength (λ_{abs}), peak emission wavelength (λ_{em}), Stokes shift ($\Delta\lambda$), oscillator strength (*f*), and *t*-index of the mOrange fluorophore analogues in water.

Fluorophore analogues	λ_{abs} (nm)	λ_{abs} (nm)[a)]	λ_{em} (nm)	λ_{em} (nm)[a)]	SS (nm)	SS (nm)[a)]	*f*	*t* index (Å)
NmOrange	410	546	452	562	42	16	0.9975	-2.164
NmOrange-3M	415		456		41		1.0075	-2.161
NmOrange-3MO	414		457		43		1.0123	-2.162
NmOrange-3N	439		525		86		0.6891	-1.542
NmOrange-35N	464		515		51		0.9094	-1.666
NmOrange-2N	401		445		44		0.9108	-1.982

[a)] Experimental data derived from previous works.[8]

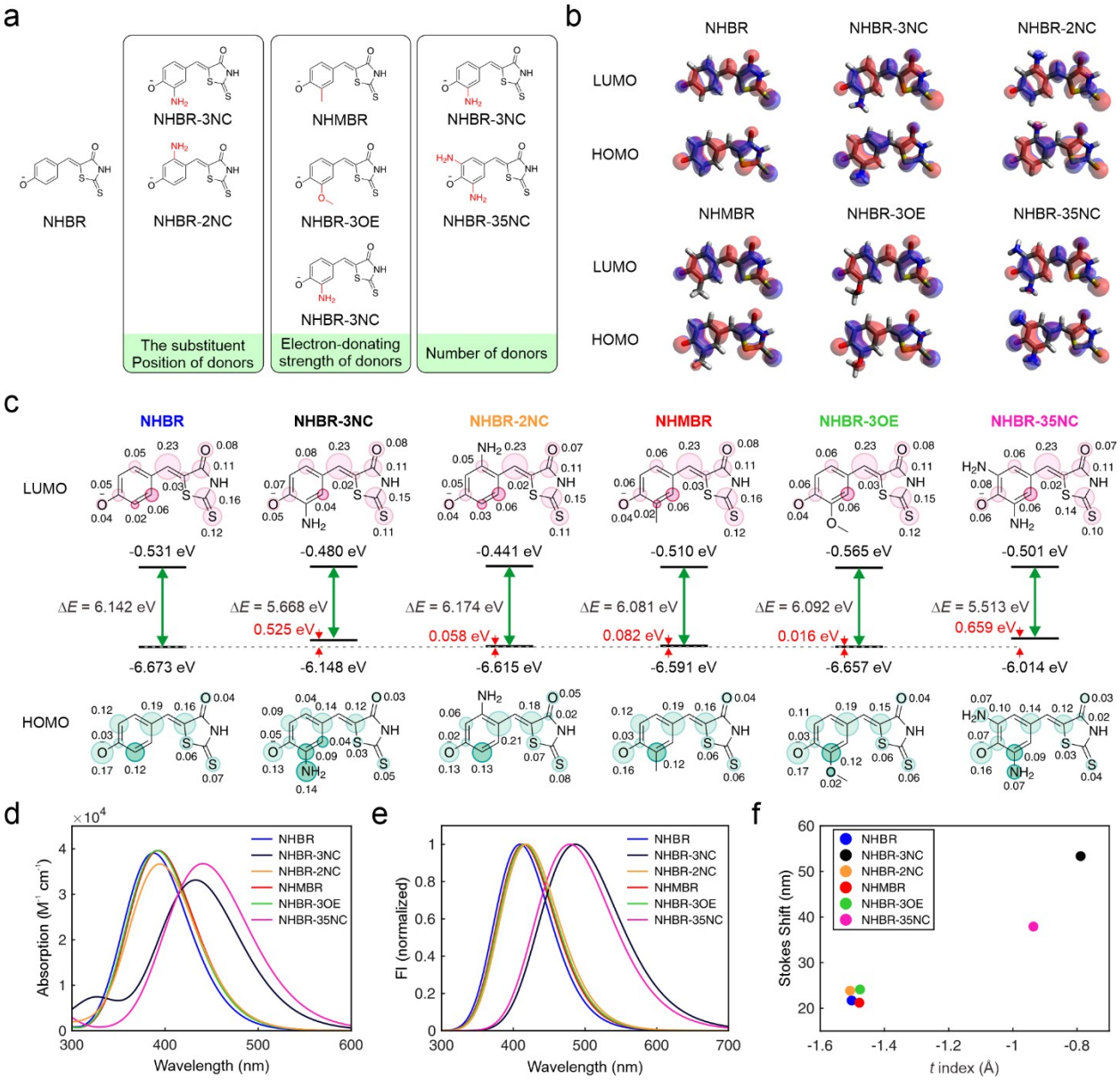

Fig. S9 (a) Chemical structures and (b) atomic contributions to the charge density distributions in the LUMO and HOMO and (c) the energy levels of HOMO and LUMO and the corresponding electronic gaps (ΔE), calculated (d) UV-vis absorption, (e) normalized emission spectra, and (f) the Stokes shifts as a function of the *t* index in the HBR analogues in water.

Table S8. Calculated/experimental peak UV-vis absorption wavelength (λ_{abs}), peak emission wavelength (λ_{em}), Stokes shift ($\Delta\lambda$), oscillator strength (*f*), and *t*-index of the HBR fluorophore analogues in water.

Fluorophore analogues	λ_{abs} (nm)	λ_{abs} (nm)[a)]	λ_{em} (nm)	λ_{em} (nm)[a)]	SS (nm)	SS (nm)[a)]	*f*	*t* index (Å)
NHBR	388		409		21		0.9665	-1.502
NHMBR	393	481	414	540	21	59	0.9776	-1.478
NHBR-3OE	392	497	416	562	24	65	0.9916	-1.476
NHBR-3NC	433		486		53		0.6688	-0.789
NHBR-35NC	441		479		38		0.861	-0.936
NHBR-2NC	395		418		23		0.8566	-1.507

[a)] Experimental data derived from previous works.[9]

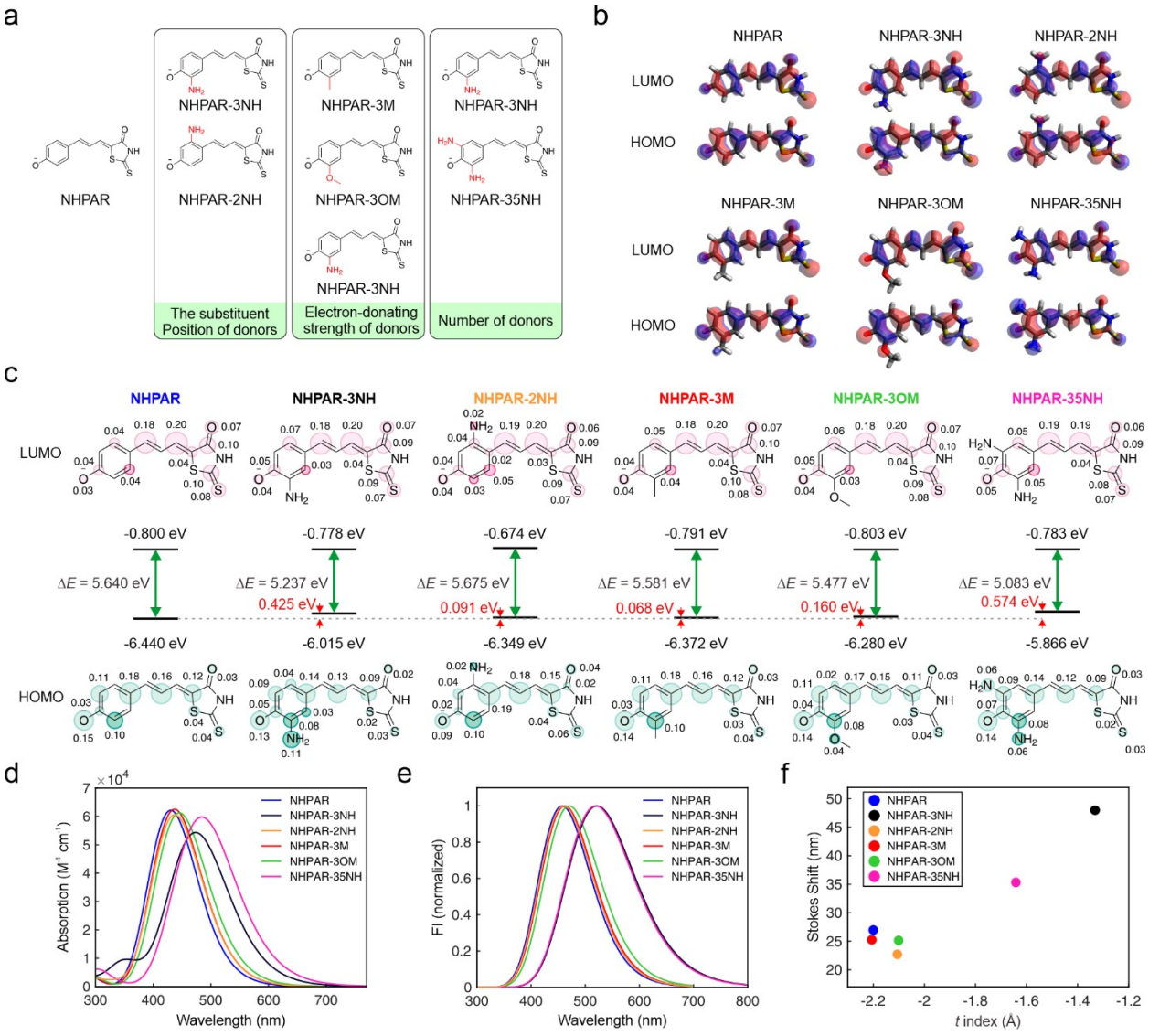

Fig. S10 (a) Chemical structures and (b) atomic contributions to the charge density distributions in the LUMO and HOMO and (c) the energy levels of HOMO and LUMO and the corresponding electronic gaps (ΔE), calculated (d) UV-vis absorption, (e) normalized emission spectra, and (f) the Stokes shifts as a function of the *t* index in the HPAR analogues in water.

Table S9. Calculated/experimental peak UV-vis absorption wavelength (λ_{abs}), peak emission wavelength (λ_{em}), Stokes shift ($\Delta\lambda$), oscillator strength (*f*), and *t*-index of the HPAR fluorophore analogues in water.

Fluorophore analogues	λ_{abs} (nm)	λ_{abs} (nm)[a)]	λ_{em} (nm)	λ_{em} (nm)[a)]	SS (nm)	SS (nm)[a)]	*f*	*t* index (Å)
NHPAR	430		457		27		1.5313	-2.200
NHPAR-3M	437		462		25		1.5365	-2.206
NHPAR-3OM	445	555	470	670	25	115	1.5135	-2.101
NHPAR-3NH	474		522		48		1.1295	-1.332
NHPAR-35NH	484		519		35		1.4035	-1.642
NHPAR-2NH	437		460		23		1.4497	-2.106

[a)] Experimental data derived from previous works.[10]

REFERENCES

1. T. Lu and F. Chen, *J. Comput. Chem.*, 2012, **33**, 580-592.

2. T. Le Bahers, C. Adamo and I. Ciofini, *J. Chem. Theory Comput.*, 2011, **7**, 2498-2506.

3. T. B. Ren, W. Xu, W. Zhang, X. X. Zhang, Z. Y. Wang, Z. Xiang, L. Yuan and X. B. Zhang, *J. Am. Chem. Soc.*, 2018, **140**, 7716-7722.

4. J. Qin, H. Yao, S. He and X. Zeng, *RSC Adv.*, 2016, **6**, 75570-75577.

5. X. Liu, Ph.D. Thesis, University of Cambridge, 2014.

6. H. Du, R. C. A. Fuh, J. Li, L. A. Corkan and J. S. Lindsey, *Photochem. Photobiol.*, 1998, **68**, 141-142.

7. Q. Fang, H. Tian, L. Yang, S. Chen, X. Liu and X. Song, *Sens. Actuators, B*, 2018, **260**, 146-155.

8. M. Drobizhev, N. S. Makarov, S. E. Tillo, T. E. Hughes and A. Rebane, *Nat. Methods*, 2011, **8**, 393-399.

9. C. Li, M.-A. Plamont, H. L. Sladitschek, V. Rodrigues, I. Aujard, P. Neveu, T. Le Saux, L. Jullien and A. Gautier, *Chem. Sci.*, 2017, **8**, 5598-5605.

10. C. Li, A. G. Tebo, M. Thauvin, M. A. Plamont, M. Volovitch, X. Morin, S. Vriz and A. Gautier, *Angew. Chem. Int. Ed.*, 2020, **132**, 17917–17923.